

Gravitational waves from the vacuum decay with LISA

Bum-Hoon Lee^{§†©1}, Wonwoo Lee^{§2}, Dong-han Yeom^{¶3}, Lu Yin^{§†4}

[§]*Center for Quantum Spacetime, Sogang University, Seoul 04107, Korea*

[†]*Department of Physics, Sogang University, Seoul 04107, Korea*

[©]*Asia Pacific Center for Theoretical Physics, Postech, Pohang 37673, Korea*

[£]*Department of Physics Education, Pusan National University, Busan 46241, Korea*

[‡]*Research Center for Dielectric and Advanced Matter Physics, Pusan National University, Busan 46241, Korea*

Abstract

We investigate the gravitational wave spectrum originating from the cosmological first-order phase transition. We compare two models: one is a scalar field model without gravitation, while the other is a scalar field model with gravitation. Based on the sensitivity curves of the LISA space-based interferometer on the stochastic gravitational-wave background, we compare the difference between the gravitational wave spectra of the former and the latter cases obtained from the bubble collision process. In particular, we numerically calculated the speed of the bubble wall before collision for the two models. We demonstrate that the difference between the amplitudes of these spectra can clearly distinguish between the two models. We expect that the LISA with Signal to Noise Ratio =10 could observe the spectrum as the fast first-order phase transition.

¹*email: bhl@sogang.ac.kr*

²*email: warrior@sogang.ac.kr*

³*email: innocent.yeom@gmail.com*

⁴*email: yinlu@sogang.ac.kr*

1 Introduction

It was reported that gravitational waves (GWs) from a binary system comprising two black holes were directly detected, in which the dominant portion of the GWs was emitted just before the collision [1, 2]. We have now opened a new window toward an unknown area that has not yet been investigated. Furthermore, we have a new opportunity to observe the past event of the universe, which took place in the regime with the strong gravitational field. Recently, GW detection has become a new challenge [3, 4], especially both in astrophysics and cosmology. Some novel topics are garnering more attention, including the GWs obtained from the pre-inflation era, inflation era [5, 6, 7, 8, 9, 10], gravitational waves that could originate from the electroweak phase transition era [11, 12, 14, 4, 15, 16], and others [17, 18, 19, 20, 21].

The origins of the stochastic gravitational waves background (SGWB) have different types of possibility. The first one is the SGWB induced nonlinearly by curvature perturbations, which is strongly related to primordial non-Gaussianity[22]. The second possibility is that of non-perturbative effects, such as sound speed resonance [23, 24] or Higgs field resonance [25, 26], which could significantly enhance cosmological gravitational waves at a certain frequency band. The cosmological first-order phase transition was first studied by the scalar field model in [27, 28]. In addition, the effects of gravity were considered in [29, 30, 31, 32, 33, 34, 35, 36, 37, 38, 39]. The authors studied the nucleation process of a vacuum bubble with $O(4)$ symmetry in the Euclidean space. Owing to the tunneling, the inside is in a lower vacuum energy state (or the broken phase), the outside is in a higher vacuum energy state (or the symmetric phase), and the transition region becomes a bubble wall. After the materialization of the vacuum bubble, the analytic continuation is conducted from Lorentzian to Euclidean signatures; eventually, the bubble expands over spacetime. Immediately after that, the procedure was applied to inflationary scenarios [40, 41, 42, 43]. In addition, the GW can be affected if multiple vacua were involved [45, 44].

In previous investigations, the authors obtained the analytic forms for the nucleation rate of a true vacuum bubble and its radius. When gravity is considered, the nucleation rate increases and the radius decreases, compared to those without gravity when the transition occurs from the de Sitter space to the flat Minkowski space [29]. As illustrated in [32], the nucleation rate could increase up to four times, provided it could have the physical meaning.

The phase transition due to the thermal effect was studied in [46, 47]. In this study, the Euclidean time becomes the inverse of the temperature; except for the time in which an $O(3)$ -symmetric vacuum bubble is generated, and it evolves in the Lorentzian spacetime. It appears difficult to simultaneously obtain the analytic forms that include both the thermal and gravity effects. Some studies have been conducted on $O(3)$ -symmetric bubble with gravitation [48, 49, 50]. We note that the nucleation rate of $O(4)$ -symmetric vacuum bubbles is more dominant than those with $O(3)$ symmetry [51].

In the thermal history of the Universe with the Standard Model of particle physics, the electroweak phase transition was not the first-order but the smooth crossover. However, we expect that the baryon asymmetry in the Universe could explain why the first-order phase

transition must occur [52, 53, 54, 55, 56, 57, 58, 59, 60]. Typically, when the electroweak phase transition was in the first-order, it was applied with its temperature, ignoring the influence of gravity. Although we cannot obtain correct analytic forms of the nucleation rate and the bubble radius with $O(4)$ -symmetry at the time of the electroweak phase transition with the finite temperature when considering the gravity, we can expect that the gravity effect will trigger more possibilities of the GW detection via space-based laser interferometry, such as Laser Interferometer Space Antenna (LISA).

LISA is a space probe that has been proposed to detect and accurately measure the GWs in the sub-Hz region from astronomical and cosmological sources. The LISA mission is designed to directly observe the GWs via laser interferometry. If an energy density more than 10^{-5} of the total energy density is converted to the gravitational radiation at the time when that is generated, LISA is sufficiently sensitive to detect the cosmological stochastic GW background that occurs in the range of energy from 0.1 TeV to 1000 TeV [3, 11]. We focus on the detection of the GWs by the bubble collision that LISA could potentially probe, which was generated by the first-order phase transition (at the electroweak scale) in the early universe.

In this study, we introduce the model-dependent parameters of the GW spectrum and solely compare the parameters of the scalar field [19] and those of the gravity cases. We describe a bubble nucleation rate and its radius when the gravity effect is strong, and demonstrate the collision phenomenon of two vacuum bubbles by adopting double-null formalism in Section 2. We compute the GW spectrum. We compare the GW spectrum from the two models with the LISA sensitivity in Section 3. Finally, we summarize our results and discuss relevant matters in Section 4.

2 Model-dependent parameters in gravitational wave spectrum

Generally, when a bubble wall eventually collides with another bubble wall, the kinetic energy disappears and converts into GWs and thermal particles. The collision of vacuum bubbles was considered for the first time in [61] without gravity, in which the collision of the two bubbles was studied. When gravity was considered, it was studied in [62]. In the bubble wall collision process, the scalar field repeatedly oscillates backward and forward between false and true vacua on the potential, while reducing the kinetic energy of the expanding bubble wall. Eventually, as the collision process gradually ends, it will settle and disappear within a true vacuum; the first-order phase transition is then completed. By adopting numerical computations, it was investigated in full general relativity [63, 64, 65, 66].

The GW spectrum from the bubble collision depends on four main parameters [12, 13]: the temperature T_* , bubble wall speed v_w , strength parameter α , and transition rate β .

T_* is the temperature when GWs are produced from bubble collisions, and the nucleation temperature $T_n \approx T_*$ is adopted for the typical transition without significant reheating. We

follow this assumption in this study and take the value $T_* \approx 100$ GeV.

The v_w parameter represents the bubble wall speed when bubble walls collide. If the bubble expands at the mean-field level, the bubble wall can accelerate without any bound, which implies that the maximum velocity (v_w) of the runaway bubble wall will quickly approach the speed of light. We will consider the numerical value of v_w .

The strength parameter α is the ratio between the vacuum energy density ρ_{vac} and that of the radiation bath ρ_{rad}^* , where $\rho_{\text{rad}}^* = g_* \pi^2 T_*^4 / 30$. Under the T_* parameter, the g_* represents the relativistic degrees of freedom in plasma. We will assume that $\alpha \approx 1$ and $g_* \approx 106.75$ in the following discussion.

The transition rate of the vacuum bubble, i.e.,

$$\beta = - \left. \frac{dB}{dt} \right|_{t=t_*},$$

will differ between the scalar field only and that with gravity cases, where B denotes the Euclidean action, which will be considered in the next Section. In the phase transition by the thermal effect, the vacuum bubble nucleation rate is not a time-independent constant. Therefore, β is non-zero, which is given by the Lorentzian time derivative of the log function of the decay rate. Because we do not know the analytic form of the nucleation rate with the $O(3)$ symmetry when considering both gravitation and temperature simultaneously, we adopt the difference between the cases with and without gravitation. We anticipate this difference to be determined by β even with the temperature effect.

The ratio of the energy density inside and outside the bubble also plays an important role in the GW spectrum, which is given by $\kappa_\phi = \rho_\phi / \rho_{\text{vac}}$. Because we do not calculate the interaction of the scalar field with plasma in this work, the energy of the false vacuum can turn into the true vacuum without loss. Hence, κ_ϕ will be considered as 1.

2.1 Decay of a metastable state and a vacuum bubble nucleation

We consider the action

$$S = \int_{\mathcal{M}} \sqrt{-g} d^4x \left[\frac{R}{2\kappa} - \frac{1}{2} \nabla_\alpha \phi \nabla^\alpha \phi - V(\phi) \right] + S_{\text{bd}}, \quad (1)$$

where $\kappa \equiv 8\pi G$, $m_p = \frac{1}{\sqrt{\kappa}} \simeq 2.44 \times 10^{18} \text{ GeV}$ represents the reduced Planck mass, $g \equiv \det g_{\mu\nu}$, and the second term on the right-hand side is the boundary term [67, 68]. The potential $V(\phi)$ has two non-degenerate minima defined as [64]:

$$V(\phi) = \frac{6V_f}{5\phi_f} \int_0^\phi \frac{\bar{\phi}}{\phi_f} \left(\frac{\bar{\phi}}{\phi_f} - 0.55 \right) \left(\frac{\bar{\phi}}{\phi_f} - 1 \right) d\bar{\phi}, \quad (2)$$

where V_f is the false vacuum energy density and ϕ_f denotes the field value of that vacuum state. The free parameter $S_f (= \sqrt{\kappa/2}\phi_f)$ can be considered as the field distance between the true and

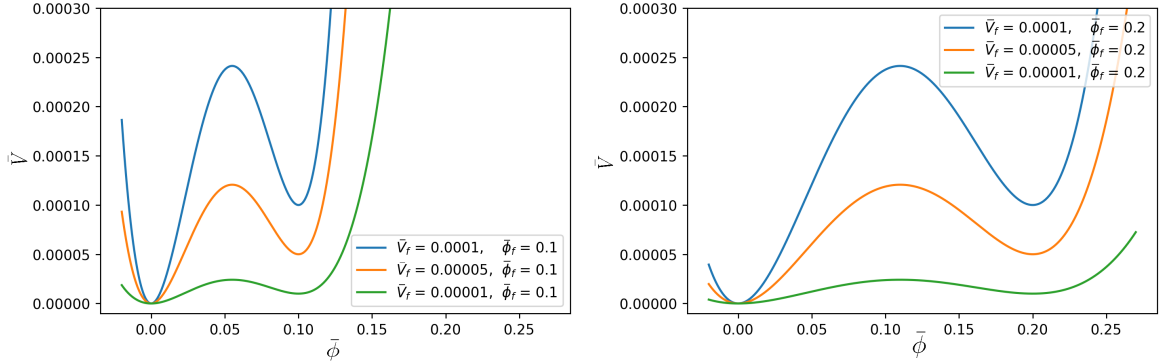


Figure 1: (color online). Potential with different value of $\bar{\phi}$ and \bar{V} from Eq. (2).

false vacuum states. For the electroweak phase transition that occurred at $T \sim 100\text{GeV}$, S_f has a value of about 10^{-16} . It is easy to understand that tunneling will be difficult to occur if S_f is too excessively large. In this study, we introduce new dimensionless scaling variables as $\bar{\phi} \equiv \phi/10^{-15}m_p$ and $\bar{V} \equiv V/(10^{-15}m_p)^4$, and then adopt the conventions $c = \hbar = 1$ for simplicity.

Figure 1 presents the potentials adopted in the numerical computations. The left figure presents $\bar{\phi}_f = 0.1$, and \bar{V}_f corresponds to 0.0001, 0.00005 and 0.00001, respectively. The right figure presents $\bar{\phi}_f = 0.2$ and \bar{V}_f exhibits the same values.

Now, we describe the vacuum bubble nucleation rate. The vacuum bubble nucleation rate per unit volume and unit time is semi-classically represented as

$$\Gamma \simeq A e^{-B}, \quad (3)$$

where the exponent B is the difference between the Euclidean action of the instanton solution (S_E^{in}) and the background action itself (S_E^{b}), i.e.,

$$B = S_E^{\text{in}} - S_E^{\text{b}}. \quad (4)$$

The prefactor A originates from the first-order quantum correction [69, 70, 71, 72]. One can further take the $O(4)$ symmetry for both the scalar field and the spacetime metric expecting its dominant contribution [51]. The Euclidean metric is given by

$$ds^2 = d\eta^2 + \rho^2(\eta) (d\chi^2 + \sin^2 \chi d\Omega_2^2). \quad (5)$$

According to [28, 29, 32], the thin-wall approximation scheme can be assumed to evaluate B . The validity of the approximation has been examined [73, 74, 75]. In this approximation, the Euclidean action can be divided into three parts: $B = B_{\text{in}} + B_{\text{wall}} + B_{\text{out}}$. The configuration of the outside the wall will not be changed before and after the bubble formation. Therefore,

$B_{\text{out}} = 0$. Hereafter, we only need to consider contributions from the wall and the inside part. The contribution of the wall is

$$B_{\text{wall}} = 2\pi^2 \bar{\rho}^3 S_o, \quad (6)$$

where the surface tension of the wall, S_o , is a constant and $\bar{\rho}$ denotes the radius of the bubble [29]. The contribution from inside the wall is given by [30, 32]

$$B_{\text{in}} = \frac{12\pi^2}{\kappa^2} \left[\frac{(1 - \frac{\kappa}{3} V_t \bar{\rho}^2)^{3/2} - 1}{V_t} - \frac{(1 - \frac{\kappa}{3} V_f \bar{\rho}^2)^{3/2} - 1}{V_f} \right]. \quad (7)$$

If the strong gravity effect is considered [32], one could obtain the relation

$$V_f - V_t = \frac{3\kappa S_o^2}{4} \quad (8)$$

in the de Sitter background. The radius of the wall $\bar{\rho}$ can be obtained by extremizing B . The above relation corresponds to $12 = \kappa \bar{\rho}_o^2 (V_f - V_t)$, where $\bar{\rho}_o (= 3S_o / (V_f - V_t))$ denotes the bubble radius in the absence of gravity. If we take $V_t = 0$, the radius and the nucleation rate of a vacuum bubble can be simplified as

$$\bar{\rho} = \frac{\bar{\rho}_o}{2}, \quad B = \frac{B_o}{4}, \quad (9)$$

where

$$B_o = \frac{27\pi^2 S_o^4}{2V_f^3} \quad (10)$$

is the nucleation rate in the absence of gravity.

For the $O(3)$ -symmetric bubble with gravitation, the nucleation rate and radius of the bubble are not clear when using the thin-wall approximation. It should be noted that a study has been conducted on the bubble with $O(3) \times O(2)$ symmetry [76]. Hereinafter, we adopt the results obtained from this study. This one provides a distinguishable difference in the exponential suppression factor B between two models, one corresponds to the event without gravitation, and the other corresponds to the event with gravitation. The inverse time duration of the phase transition corresponding to the nucleation rate of an $O(3)$ -symmetric bubble is given by [77, 12]

$$\beta \equiv - \left. \frac{dB}{dt} \right|_{t=t_*} \simeq \frac{\dot{\Gamma}}{\Gamma}. \quad (11)$$

Hence, we obtain the following relation of β at the time of the bubble collision:

$$\beta_S \approx 4\beta_{S+G}, \quad (12)$$

where the subscript “ S ” denotes the event without gravitation, while “ $S+G$ ” denotes the event with gravitation. This result is one of the reasons why the GWs spectrum can be distinguished between the scalar field only and that with gravity cases (Section 3), although the real value of the ratio will be smaller than 4 times.

2.2 Bubble collision

Now, we consider two identical vacuum bubbles with a preferred axis; then, the geometry is reduced to the $O(2, 1)$ symmetry by the existence of the axis [61, 62, 78, 79]. To describe the bubble collision phenomenon, we adopt the double-null formalism [64, 80]. We choose the metric ansatz for the hyperbolic symmetry:

$$ds^2 = -\alpha^2(u, v)dudv + r^2(u, v)dH^2, \quad (13)$$

where r denotes a timelike coordinate, $dH^2 = d\chi^2 + \sinh^2\chi d\varphi^2$, while u and v correspond to the left- and right-going null directions, respectively. Note that typical black hole type solutions correspond to $m < 0$; hence, we are interested in the case with $m < 0$. Accordingly, we follow the procedure with some conventions and equations of motion used in [64]. The mathematical and numerical details of the simulations are summarized in Appendix.

In this paper, we briefly describe initial conditions along initial $u = 0$ and $v = 0$ surfaces.

Initial $v = 0$ surface: we adopt

$$S(u, 0) = \begin{cases} \bar{\phi}_f & u < u_{\text{shell}}, \\ \left[\bar{\phi}_t - \bar{\phi}_f \right] G(u) + \bar{\phi}_t & u_{\text{shell}} \leq u < u_{\text{shell}} + \Delta u, \\ \bar{\phi}_t & u_{\text{shell}} + \Delta u \leq u, \end{cases} \quad (14)$$

where $G(u)$ is a function that pastes from 1 to 0 in a smooth manner:

$$G(u) = 1 - \sin^2 \left[\frac{\pi(u - u_{\text{shell}})}{2\Delta u} \right]. \quad (15)$$

Initial $u = 0$ surface: We choose

$$S(0, v) = \begin{cases} \bar{\phi}_f & v < v_{\text{shell}}, \\ \left[\bar{\phi}_f - \bar{\phi}_t \right] G(v) - \bar{\phi}_t & v_{\text{shell}} \leq v < v_{\text{shell}} + \Delta v, \\ \bar{\phi}_t & v_{\text{shell}} + \Delta v \leq v, \end{cases} \quad (16)$$

where

$$G(v) = 1 - \sin^2 \left[\frac{\pi(v - v_{\text{shell}})}{2\Delta v} \right]. \quad (17)$$

In order to specify a false vacuum background, we impose $r(0, 0) = r_0$ and $S(0, 0) = \bar{\phi}_f$. The two parameters r_0 and $\bar{\phi}_f$ are free parameters and the value of $\bar{\phi}_f$ can be considered as the field distance from the true to false vacuum. As a model parameter, we consider $\bar{\phi}_f = 0.1$ and 0.2 in this work. In addition, we select $r_0 = 1$ in the next calculation. Regarding the detailed meanings of the boundary conditions and model parameters, refer to Appendix and [64].

Figures 2 and 3 present the numerical results of the bubble collisions. The red-colored region indicates large vacuum energy while the blue-colored region represents the region of low

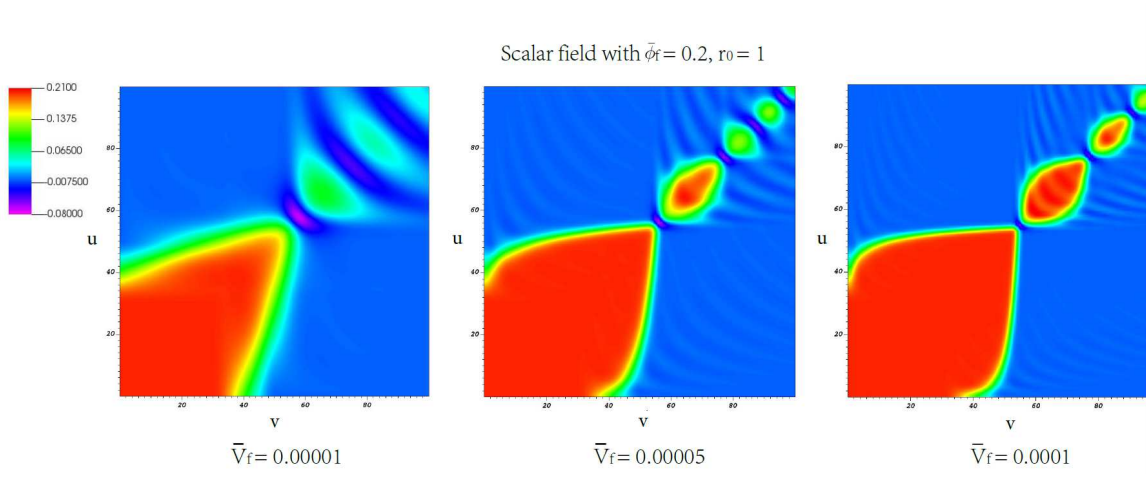


Figure 2: (color online). Bubble percolation with spherical symmetry: for $\bar{\phi}_f = 0.2$ and $r_0 = 1$ at scalar field with $\bar{V}_f = 0.00001, 0.00005,$ and $0.0001,$ respectively.

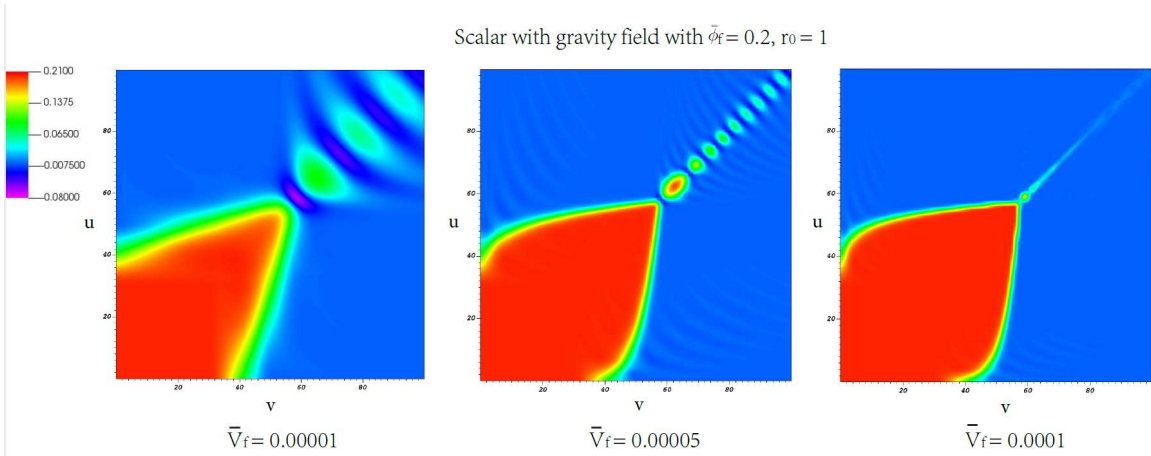


Figure 3: (color online). Bubble percolation with spherical symmetry: for $\bar{\phi}_f = 0.2$ and $r_0 = 1$ at scalar with gravity field with $\bar{V}_f = 0.00001, 0.00005,$ and $0.0001,$ respectively.

Table 1: Velocity of bubble wall before collision in scalar with gravity field and scalar field with $\bar{\phi}_f = 0.2$.

| Value of v_w | $\bar{V}_f = 0.00001$ | $\bar{V}_f = 0.00005$ | $\bar{V}_f = 0.0001$ |
|---------------------------|-----------------------|-----------------------|----------------------|
| Scalar field | 0.895 | 0.867 | 0.620 |
| Scalar with gravity field | 0.875 | 0.761 | 0.578 |

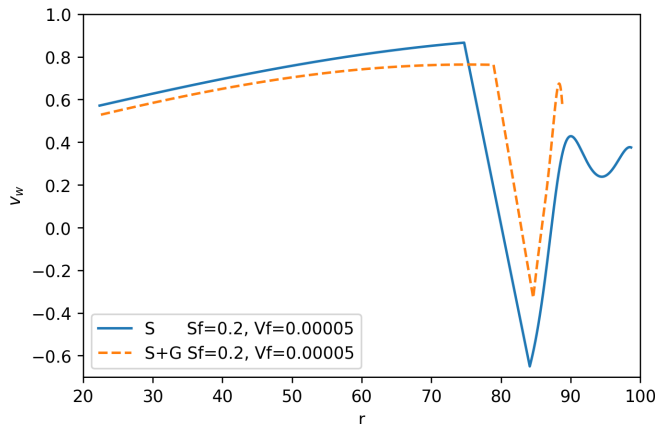


Figure 4: (color online). Time evolution of the bubble wall velocity. The r is a timelike coordinate. The setting of potential are same in scalar-only and scalar with gravity cases, which have $\bar{\phi}_f = 0.2$, $r_0 = 1$, and $\bar{V}_f = 0.00005$, respectively.

potential energy. We can consider them as false vacuum and true vacuum regions, respectively. As the wall oscillates, the oscillating field amplitudes decrease (upper right), and eventually, the wall disappears (lower left). As the tension of the shell increases, the initial expansion of the shell gradually slows down. For the scalar field with the gravity case, the field oscillation becomes faster than that of the scalar field without the gravity case.

We also obtain the velocity of the bubble wall before collision from Figures 2 and 3. We approximately considered the slope of the yellow line and calculated the velocity by

$$v_w = \frac{\Delta v - \Delta u}{\Delta v + \Delta u}. \quad (18)$$

The numerical results for v_w in different potentials are presented in Table 1.

The Figure 4 presents the velocity evolution of the bubble wall for the scalar field and that with the gravity cases. From the same set of potentials (including $\bar{\phi}_f = 0.2$ and $\bar{V}_f = 0.00005$), the scalar-only case has the faster velocity of the bubble wall than that with gravity case before the bubble collision. The abscissa r here is defined by $r = v+u$, which could not correspond with real-time in cosmology. Before the collision, the numerical result of velocity exhibits $v_w = 0.867$ at approximately $r = 75$ for the scalar field case, while v_w equals to 0.761 for the case with

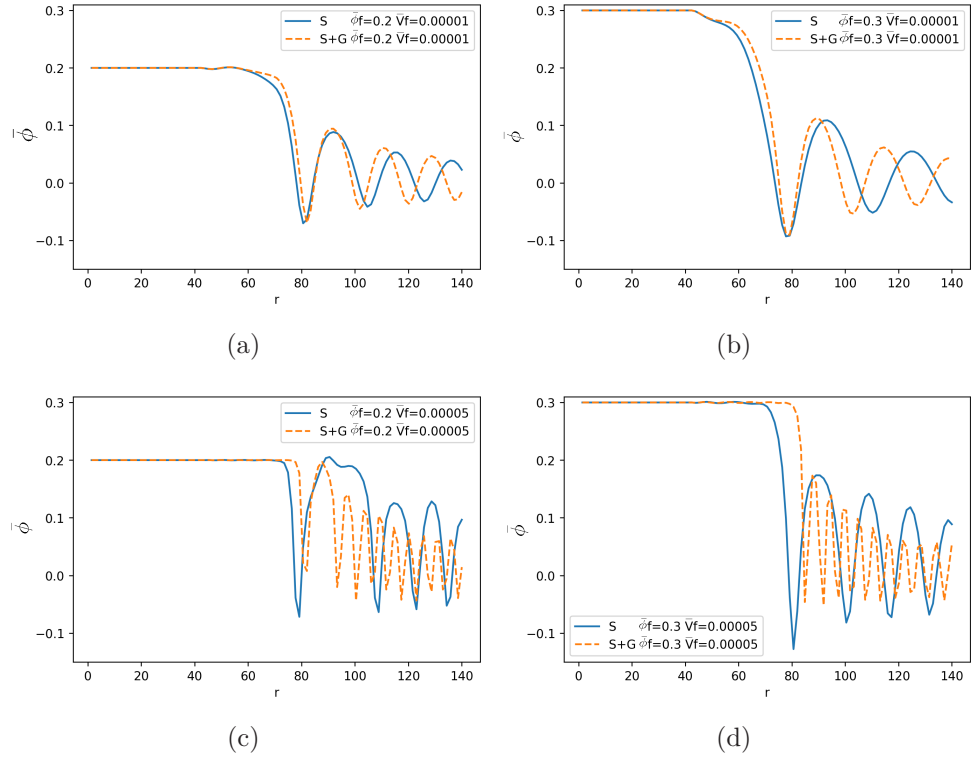


Figure 5: (color online). Time evolution of the potential for one point from the false vacuum. The “ $S + G$ ” means the scalar with gravity field and the “ S ” is the scalar field only case.

gravity, as illustrated in Table 1. The label “ S ” in the figure implies the scalar-only field case, while the adopted “ $S + G$ ” represents the scalar with gravity case. Another information we can confirm from this figure is that the case of “ $S + G$ ” exhibits a later collision time than the scalar-only case, and the frequency of the oscillation is faster than that in the scalar-only case.

To understand the time evolution for the vacuum state of the outside of the wall as the scalar field on the potential, we select one point in the false vacuum and compare the oscillation of the point in different cases (refer to 5). When the two bubbles collide, the potential for this point will turn to the true vacuum. Then, the potential will oscillate back to zero. In the same sub-figure of Figure 5, the initial potential is also identical for the “ S ” and “ $S + G$ ” cases. The comparative is interesting that the moment of two bubbles collision in “ $S + G$ ” will always be later than the scalar-only case. In addition, the potential in the “ $S + G$ ” case will oscillate quicker than that in the scalar-only case. We can compare the potential by different values of $\bar{\phi}_f$ in (a) and (b) (also (c) and (d)). For (a) and (c) (also (b) and (d)), we can observe that the frequency of oscillation will significantly depend on the parameter \bar{V}_f . The higher value of \bar{V}_f will lead to a faster oscillation.

3 Computation of gravitational wave spectrum

One of the most important assumptions for the GW spectrum from bubble collision is that GW does not depend on the form of the potential [81]. In this section, we provide a comprehensive general derivation process for the GW spectrum.

3.1 Formalism of gravitational wave spectrum

Firstly, we allow the background spacetime to be dynamical, which implies that we would like to define GWs as perturbations over some curved and dynamical background metric $\bar{g}_{\mu\nu}$. Therefore, one can write $g_{\mu\nu} = \bar{g}_{\mu\nu} + h_{\mu\nu}$ with $|h_{\mu\nu}| \ll 1$ [82]. The “coarse-grained” form of the Einstein equations can be given by

$$\bar{R}_{\mu\nu} - \frac{1}{2}\bar{g}_{\mu\nu}\bar{R} = \frac{8\pi G}{c^4}(\bar{T}_{\mu\nu} + t_{\mu\nu}), \quad (19)$$

where the equation determines the dynamics of $\bar{g}_{\mu\nu}$, which is the long-wavelength part of the metric. $\bar{T}_{\mu\nu}$ is the matter energy-momentum tensor in terms of the long-wavelength, and the tensor $t_{\mu\nu}$ here does not depend on the external matter, but on the gravitational field itself. These two tensor terms are also quadratic in terms of $h_{\mu\nu}$.

With the gauge invariant energy density in terms of the amplitudes h_+^2 and h_\times^2 setting as $t^{00} = \frac{c^2}{16\pi G}\langle \dot{h}_+^2 + \dot{h}_\times^2 \rangle$, we compute the corresponding energy flux straightforward. Because the energy-momentum tensor can be expressed by the GWs, the total energy flowing through the surface of dA is written as

$$\frac{dE}{dA} = \frac{c^3}{16\pi G} \int_{-\infty}^{+\infty} dt \langle \dot{h}_+^2 + \dot{h}_\times^2 \rangle. \quad (20)$$

In the next calculation, we focus on the determination of the GW spectrum. Based on Eq. (20), the fundamental equation for the GW spectrum can be considered with the angle $d\Omega$ as

$$\begin{aligned} \frac{dE}{d\Omega} &= \frac{r^2 c^3}{16\pi G} \int_{-\infty}^{+\infty} dt \left(\dot{h}_+^2 + \dot{h}_\times^2 \right) \\ &= \frac{G}{2\pi^2 c^7} \Lambda_{ij,kl}(\hat{\mathbf{k}}) \int_0^{+\infty} d\omega \omega^2 \tilde{T}_{ij} \left(\omega, \frac{\omega \hat{\mathbf{k}}}{c} \right) \tilde{T}_{kl}^* \left(\omega, \frac{\omega \hat{\mathbf{k}}}{c} \right), \end{aligned} \quad (21)$$

where $d\omega$ indicates the frequency interval. The energy spectrum per solid angle is given by [83]

$$\frac{d^2 E}{d\omega d\Omega} = 2G\omega^2 \Lambda_{ij,kl}(\hat{\mathbf{k}}) \tilde{T}_{ij}(\hat{\mathbf{k}}, \omega) \tilde{T}_{kl}^*(\hat{\mathbf{k}}, \omega), \quad (22)$$

where $\Lambda_{ij,kl}$ in Eq. (22) is the GWs' projection tensor, and the full form is expressed as [84]:

$$\Lambda_{ij,kl}(\hat{\mathbf{k}}) = \delta_{il}\delta_{jm} - 2\hat{\mathbf{k}}_j\hat{\mathbf{k}}_m\delta_{il} + \frac{1}{2}\hat{\mathbf{k}}_i\hat{\mathbf{k}}_j\hat{\mathbf{k}}_l\hat{\mathbf{k}}_m - \frac{1}{2}\delta_{ij}\delta_{lm} + \frac{1}{2}\hat{\mathbf{k}}_l\hat{\mathbf{k}}_m + \frac{1}{2}\delta_{lm}\hat{\mathbf{k}}_i\hat{\mathbf{k}}_j. \quad (23)$$

The instantaneously radiated power is significantly more useful because the total radiated energy is formally divergent. In the Fourier space, the stress-energy tensor is

$$T_{ij}(\hat{\mathbf{k}}, \omega) = \frac{1}{2\pi} \int dt e^{i\omega t} \sum_n \int_{S_n} d\Omega \int dr r^2 e^{-i\omega \hat{\mathbf{k}} \cdot (\mathbf{x}_n + r\hat{\mathbf{x}})} T_{ij,n}(r, t), \quad (24)$$

where the \mathbf{x}_n is the position of the bubble in the nucleation, and S_n is the un-collided region of the n -th bubble.

In the first-order phase transition, $1/\beta$ denotes the duration roughly, which will be set as the frequency of GWs. Accordingly, we can write $\omega \approx \beta$ for the characteristic frequency of the radiation. Meanwhile, we also consider the single bubble radius as R in the below function, and this can determine the scaling of the radiation spectrum amplitude:

$$\int_0^{R_n} dr r^2 T_{ij}(r, t) \approx \frac{1}{3} \hat{\mathbf{x}}_i \hat{\mathbf{x}}_j R_n^3 \kappa_\phi \epsilon = \frac{1}{4} \hat{\mathbf{x}}_i \hat{\mathbf{x}}_j R_n^3 \kappa_\phi \alpha \omega_1, \quad (25)$$

where κ_ϕ is the efficiency factor introduced previously and the subscript 1 denotes the quantity in the symmetric phase [85].

We ignore the $e^{-i\omega \hat{\mathbf{k}} \cdot (\mathbf{x}_n + r\hat{\mathbf{x}})}$ term as 1 in Eq. (24) and consider the length scale as $R \simeq v/\beta$. With the number of bubble setting as N , we can obtain the approximation of GW spectrum in the bubble collision time as

$$\frac{dE}{d\omega} \propto NG (R^3 \kappa_\phi \epsilon)^2. \quad (26)$$

In addition, this equation can be simplified as $\frac{1}{E_{vac}} \frac{dE}{d\omega} \propto Gv^3 \kappa_\phi^2 \alpha \frac{\omega_1}{\beta^3}$.

The fraction of energy liberated into the GW radiation per frequency octave is

$$\Omega_{\text{GW}*} = \omega \frac{dE_{\text{GW}}}{d\omega} \frac{1}{E_{\text{tot}}} = \kappa_\phi^2 \left(\frac{H_*}{\beta} \right)^2 \left(\frac{\alpha}{\alpha + 1} \right)^2 \Delta(\omega/\beta, v_b), \quad (27)$$

where E_{vac} denotes the total vacuum energy in the sample volume, which is given as $E_{\text{vac}} \simeq NR^3\epsilon$ and the Δ is a dimensionless function term, which can be defined as $\Delta\left(\frac{\omega}{\beta}, v_b\right) = \frac{\omega^3}{\beta^3} \frac{3v_b^6\beta^5}{2\pi V} \int d\hat{k} \Lambda_{ij,lm} C_{ij}^* C_{lm}$, in which one can refer to Ref. [83] for the definition of C_{ij} . The star subscript (*) refers to the means at the time of the first order phase transition happened. The Hubble parameter at the time of the phase transition is

$$H_*^2 = \frac{8\pi G\rho_{\text{rad}}}{3} = \frac{8\pi^3 g_* T_*^4}{90m_{\text{Pl}}^2}. \quad (28)$$

One can obtain $\int d\hat{k} \Lambda_{ij,lm} C_{ij}^* C_{lm} \propto N\beta^{-8} \propto \frac{V}{v_b^3\beta^5}$ can be obtained in the quadrupole approximation, if the integration is performed over a large volume V of the Universe.

After obtaining the spectrum of $\Omega_{\text{GW}*}$ in the moment of bubble collision, we are going to calculate the corresponding signal in the present Universe. We consider that the entropy per comoving volume is always the same in the history of the Universe, and the relationship can be set as $S \propto R^3 g(T) T^3$. At the temperature T_* , the number of relativistic degrees of freedom was expressed in $g(T_*)$. Hence, we can obtain

$$\frac{R_*}{R_0} = 8.0 \times 10^{-14} \left(\frac{100}{g_*} \right)^{1/3} \left(\frac{1\text{GeV}}{T_*} \right), \quad (29)$$

where $g_* = 106.75$ was considered at an electroweak scale.

The f_* parameter denotes the characteristic frequency at the transition, and the characteristic frequency f_0 today can be considered as [83]

$$f_0 = f_* \left(\frac{R_*}{R_0} \right) = 1.65 \times 10^{-7} \text{ Hz} \left(\frac{f_*}{H_*} \right) \left(\frac{T_*}{1\text{GeV}} \right) \left(\frac{g_*}{100} \right)^{1/6}, \quad (30)$$

$$\Omega_{\text{GW}} h^2 = \Omega_{\text{GW}*} \left(\frac{R_*}{R_0} \right)^4 H_*^2 = 1.67 \times 10^{-5} \left(\frac{100}{g_*} \right)^{1/3} \Omega_{\text{GW}*}, \quad (31)$$

where h is the current Hubble parameter result. Note that the quantity $\Omega_{\text{GW}} h^2$ is independent of the actual Hubble expansion rate. Hence, that quantity is often adopted, rather than Ω_{GW} alone.

We can parameterize the spectrum of the GWs (the energy density spectrum) from bubble collisions by

$$\Omega_{\text{GW}}(f) h^2 = 1.67 \times 10^{-5} \left(\frac{100}{g_*} \right)^{1/3} \left(\frac{H_*}{\beta} \right)^2 \left(\frac{\kappa_\phi \alpha}{\alpha + 1} \right)^2 \Delta S(f) \quad (32)$$

where the parameter β/H_* controls the GW signal. A small value of β/H_* means the fast first-order phase transition. $\Delta = \frac{0.11v_b^3}{0.42+v_b^2}$ is obtained from the numerical result in [83] and $S(f) = \frac{3.8(f/f_0)^{2.8}}{1+2.8(f/f_0)^{3.8}}$ parameterizes the spectral shape of the GW radiation.

3.2 Gravitational wave spectrum with LISA

In this study, we solely focus on the contribution of the scalar field without the sound wave and turbulence. We compare the GW spectra both from the scalar field model and that with gravity by the LISA sensitivity. The bubble collisions will produce a stochastic background of GWs. The stochastic backgrounds are random GW signals due to the superposition of many independent uncorrelated sources that cannot be resolved individually [87], which can be tested by the space-based interferometer LISA. The sensitivity result of LISA for a stochastic gravitational-wave background was also presented in Figure 6. The redline represents the sensitivity curve derived from the noise model we adopt in LISA. We consider the sensitivity of LISA with several parameters [98, 99]. We used an observation time of 4 years with 75% efficiency, meaning that we set $T = 3$ years. In the figure, the Signal to Noise Ratio (SNR) was in fact at approximately 7, which confirms that the choice $\text{SNR} \approx 10$ for the gravitational wave signal is feasible, as depicted by the purple line and also found in [100].

The comparison of results can be PRESENTED in Fig.6. In this figure, the β_s/H_* values are 50, 100, 800, and 1500, respectively. Meanwhile, the corresponding values for cases with gravity are 12.5, 25, 200, and 375, which are the same as the relationship in Eq. (12). The larger value of β_s/H_* implies the relatively slow first-order phase transition. In slower first-order phase transitions, most of the vacuum energy is released into the acceleration of the bubble walls [14]. The value of T_* is 100 GeV, and for v_w , we adopted the case for $\bar{\phi}_f = 0.2$ and $\bar{V}_f = 0.00005$.

These results are easy to read from Figure 6. First, the GW spectrum for the scalar with gravity case has a larger amplitude than that in the scalar-only case at the same frequency. When gravity is considered, the peak frequency shifts to the upper left. In particular, when $\beta_s/H_* = 1500$, the $S + G$ case can be tested by the LISA observation; however, the scalar-only case exhibits our range. This suggests that the scalar with the gravity case will be tested easier than the scalar-only case in the same original setting, which implies the possibility for distinguishing the two cases in the LISA observation. This result is mainly based on the different contributions from the β parameter.

4 Summary and discussions

In this study, we investigated the gravitational wave spectrum originating from the bubble collision and compared the difference of the parameters $\bar{\phi}$, β , and v_w in the scalar-only field and that with gravity field cases. We compared the evolution of v_w from numerical simulation. In the same initial distance, the v_w in scalar with gravity case will always be smaller than the

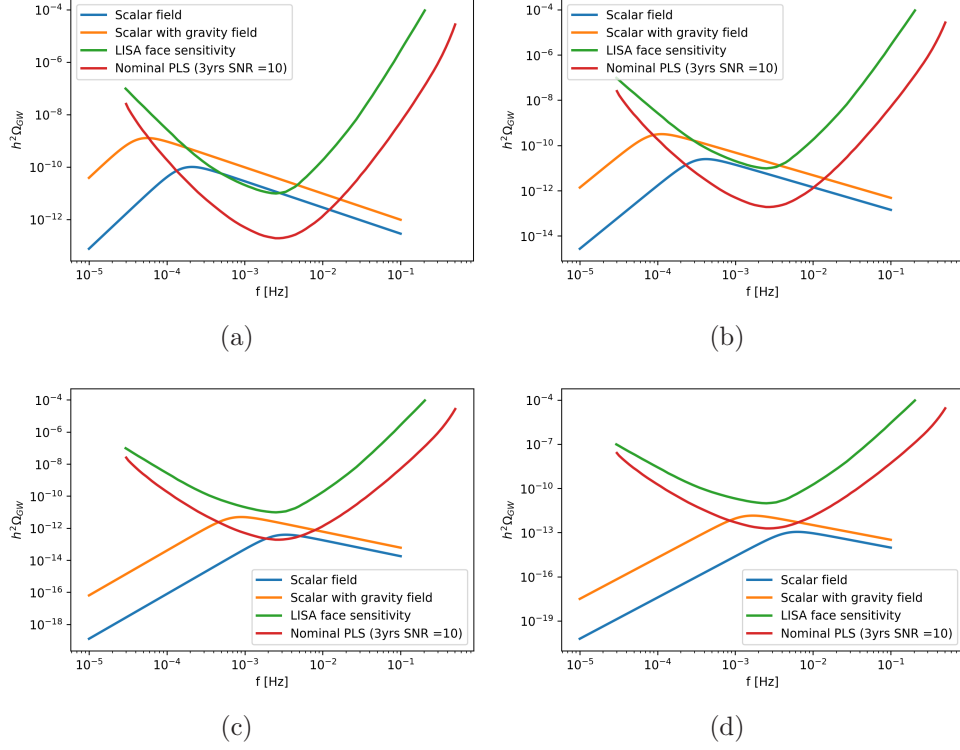


Figure 6: (color online). Gravitational wave spectrum considered the contribution from bubbles with $\bar{\phi}_f = 0.2$ and $\bar{V}_f = 0.00005$. The value of β_s/H_* are 50, 100, 800, and 1500, respectively. The broken power law sensitivity curve derived from the noise model we adopt (green curve) and the corresponding PLS for $T = 3$ yr with $\text{SNR} = 10$ (red curve) $v_w^S = 0.867$ and $v_w^{S+G} = 0.761$ in this figure.

scalar-only case, and v_w will also be reduced with a larger potential energy difference. The ratio β_S/β_{S+G} is approximately 4 times in the Minkowski space, and this difference in β triggered the main differences in the peak and the amplitude of the gravitational wave spectrum. In the comparison of gravitational wave spectrum produced from the two fields in the vacuum-only state, we can observe that the amplitude in the scalar field case with gravity can exhibit have a larger value than that in the scalar-only field case. With this higher amplitude, we expected that the LISA with SNR=10 could observe the spectrum as the fast first-order phase transition. Compared to previous studies that did not consider the effect of gravitation, our present study considered the effect of gravitation. At the electroweak phase transition, it may be believed that the effect was not significant, but we considered the case when the effect was maximum. Hence, we expect that the gravitational wave spectrum will be relatively above, but not significantly in line without the gravitational effect. However, that will be between the line without the gravitational effect and that with the strong one. We would like to emphasize that we have provided an upper bound in this paper, even though the gravitational effect was negligible at the electroweak phase transition era.

In one of our previous works, we investigated gravitational waves from cosmic bubble collisions, in which time-domain gravitational waveforms were directly obtained by integrating the energy-momentum tensors over the volume of the wave sources [78]. Both the time- and frequency-domains of the gravitational wave analysis in the context of the bubble collisions might be interesting not only theoretical but also from the experimental perspective. Based on this work, along with the previous work, it is believed that they will be in a mutually complementary relationship to investigate the cosmological gravitational wave spectrum.

It will also be interesting to study bubble collisions not only in Einstein's gravity but also in various other models including string-inspired scenarios [88, 89, 90] or modified gravity models [91, 92, 93]. We leave these possible directions for future research topics.

Acknowledgments

BHL (2020R1F1A1075472), DY (2021R1C1C1008622, 2021R1A4A5031460), and WL (2016R1D1A1B01010234) were supported by the National Research Foundation of Korea. LY was supported by the Basic Science Research Program (2020R1A6A1A03047877) of the National Research Foundation of Korea funded by the Ministry of Education through Center for Quantum Spacetime (CQUeST) of Sogang University. The authors thank the organizers for their hospitality at the 17th Italian-Korean Symposium for Relativistic Astrophysics in Kunsan National University, 02- 06 August 2021. The authors also thank Hyeong-Chan Kim and Youngone Lee for their hospitality during our visit to Korea National University of Transportation; Hoon Soo Kang, Keun-Young Kim, Chanyong Park, Yun-Seok Seo, and Hyun Seok Yang to GIST; Seoktae Koh to Jeju National University. BHL is grateful to APCTP for their hospitality during his visit. We appreciate the discussion from Gianmassimo Tasinato and Ke-Pan Xie.

Appendix: brief review of the double-null simulation

The generic review of the double-null simulation is in Ref. [80, 94]. For convenience, we first define

$$\sqrt{4\pi}\phi \equiv S. \quad (33)$$

In addition, we define

$$h \equiv \frac{\alpha_{,u}}{\alpha}, \quad d \equiv \frac{\alpha_{,v}}{\alpha}, \quad f \equiv r_{,u}, \quad g \equiv r_{,v}, \quad W \equiv S_{,u}, \quad Z \equiv S_{,v}, \quad (34)$$

to present all equations as a set of first-order partial differential equations. In particular, for examples to study vacuum bubbles in double-null simulations, refer to Refs. [95, 96, 97].

After a simple derivation, we obtain the Einstein tensor components

$$G_{uu} = -\frac{2}{r}(f_{,u} - 2fh), \quad (35)$$

$$G_{uv} = \frac{1}{2r^2}(4rf_{,v} - \alpha^2 + 4fg), \quad (36)$$

$$G_{vv} = -\frac{2}{r}(g_{,v} - 2gd), \quad (37)$$

$$G_{\chi\chi} = -4\frac{r^2}{\alpha^2}\left(d_{,u} + \frac{f_{,v}}{r}\right), \quad (38)$$

and the energy-momentum tensor components

$$T_{uu}^\phi = \frac{1}{4\pi}W^2, \quad (39)$$

$$T_{uv}^\phi = \frac{\alpha^2}{2}V(S), \quad (40)$$

$$T_{vv}^\phi = \frac{1}{4\pi}Z^2, \quad (41)$$

$$T_{aa}^\phi = \frac{r^2}{2\pi\alpha^2}WZ - r^2V(S). \quad (42)$$

Therefore, the Einstein equations are as follows:

$$f_{,u} = 2fh - 4\pi GrT_{uu}^\phi, \quad (43)$$

$$g_{,v} = 2gd - 4\pi GrT_{vv}^\phi, \quad (44)$$

$$f_{,v} = g_{,u} = -\kappa\frac{\alpha^2}{4r} - \frac{fg}{r} + 4\pi GrT_{uv}^\phi, \quad (45)$$

$$h_{,v} = d_{,u} = -\frac{2\pi G\alpha^2}{r^2}T_{aa}^\phi - \frac{f_{,v}}{r}. \quad (46)$$

Here, G is the gravitational constant; if we take $G = 0$, this corresponds to the scalar-only field case without gravitational back-reactions. The scalar field equation becomes

$$Z_{,u} = W_{,v} = -\frac{fZ}{r} - \frac{gW}{r} - \pi\alpha^2 V'(S). \quad (47)$$

By comparing with the static metric, we can determine a principle to provide the physical boundary condition. The static metric form is

$$ds^2 = -N^2(r)dt^2 + \frac{dr^2}{N^2(r)} + r^2 dH^2, \quad (48)$$

where

$$N^2 = -\left(1 + \frac{2M}{r} + \frac{8\pi V r^2}{3}\right). \quad (49)$$

For typical hyperbolically symmetric cases, t is the space-like parameter and r denotes the time-like parameter. By comparing to the double-null metric, we obtain

$$N^2 = -\frac{4r_{,u}r_{,v}}{\alpha^2}. \quad (50)$$

Hence, one can choose $r_{,u} > 0$ and $r_{,v} > 0$. The Misner-Sharp mass function in the double-null coordinate is

$$m(u, v) = -\frac{r}{2} \left(1 - \frac{4r_{,u}r_{,v}}{\alpha^2} + \frac{8\pi V}{3} r^2\right). \quad (51)$$

Note that usual black hole type solutions in Minkowski vacuum will occur for $m < 0$ limit; hence, in this study, we are interested in $m \leq 0$.

Finally, boundary conditions along initial $u = 0$ and $v = 0$ surfaces are assigned as follows.

$v = 0$ surface: We first choose $S(u, 0)$. Then, we know $W(u, 0) = S_{,u}(u, 0)$. From this, $h(u, 0)$ is given from Equation (43), since $f_{,u} = 0$ along the in-going null surface. Then, using $h(u, 0)$, we obtain $\alpha(u, 0)$. In addition to them, we further obtain d from Equation (46), g from Equation (45), and Z from Equation (47).

$u = 0$ surface: we first adopt $S(0, v)$. Then, we obtain $d(0, v)$ from Equation (44), as $g_{,v}(0, v) = 0$. By integrating d along v , we have $\alpha(0, v)$. In addition, we further obtain h from Equation (46), f from Equation (45), and W from Equation (47).

We used the 2nd-order Runge-Kutta method. The consistency and the convergence checks were analyzed in Ref. [64].

References

- [1] B. P. Abbott *et al.* [LIGO Scientific and Virgo Collaborations], Phys. Rev. Lett. **116**, no. 24, 241103 (2016) [arXiv:1606.04855 [gr-qc]].
- [2] B. P. Abbott *et al.* [LIGO Scientific and VIRGO Collaborations], Phys. Rev. Lett. **118**, no. 22, 221101 (2017) [arXiv:1706.01812 [gr-qc]].
- [3] P. Amaro-Seoane *et al.*, GW Notes **6**, 4 (2013) [arXiv:1201.3621 [astro-ph.CO]].
- [4] C. Caprini *et al.*, JCAP **2003**, 024 (2020) [arXiv:1910.13125 [astro-ph.CO]].
- [5] A. A. Starobinsky, JETP Lett. **30**, 682 (1979) [Pisma Zh. Eksp. Teor. Fiz. **30**, 719 (1979)].
- [6] S. Koh, S. P. Kim and D. J. Song, JHEP **0412**, 060 (2004) doi:10.1088/1126-6708/2004/12/060 [gr-qc/0402065].
- [7] N. Bartolo *et al.*, JCAP **1612**, 026 (2016) [arXiv:1610.06481 [astro-ph.CO]].
- [8] H. Di and Y. Gong, JCAP **1807**, 007 (2018) [arXiv:1707.09578 [astro-ph.CO]].
- [9] S. Koh, B. H. Lee and G. Tumurtushaa, Phys. Rev. D **98**, no. 10, 103511 (2018) [arXiv:1807.04424 [astro-ph.CO]].
- [10] D. Huang and L. Yin, Phys. Rev. D **100**, no. 4, 043538 (2019) doi:10.1103/PhysRevD.100.043538 [arXiv:1905.08510 [hep-ph]].
- [11] P. Binetruy, A. Bohe, C. Caprini and J. F. Dufaux, JCAP **1206**, 027 (2012) [arXiv:1201.0983 [gr-qc]].
- [12] C. Caprini *et al.*, JCAP **1604**, 001 (2016) [arXiv:1512.06239 [astro-ph.CO]].
- [13] X. Wang, F. P. Huang and X. Zhang, [arXiv:2011.12903 [hep-ph]].
- [14] R. G. Cai, M. Sasaki and S. J. Wang, JCAP **1708**, 004 (2017) [arXiv:1707.03001 [astro-ph.CO]].
- [15] R. Jinno and M. Takimoto, JCAP **1901**, 060 (2019) [arXiv:1707.03111 [hep-ph]].
- [16] K. Schmitz, JHEP **2101**, 097 (2021) doi:10.1007/JHEP01(2021)097 [arXiv:2002.04615 [hep-ph]].
- [17] A. Vilenkin, Phys. Lett. **107B**, 47 (1981).
- [18] G. Barenboim and W. I. Park, Phys. Lett. B **759**, 430 (2016) [arXiv:1605.03781 [astro-ph.CO]].

- [19] M. Lewicki and V. Vaskonen, Phys. Dark Univ. **30**, 100672 (2020) [arXiv:1912.00997 [astro-ph.CO]].
- [20] H. K. Guo, K. Sinha, D. Vagie and G. White, JCAP **2101**, 001 (2021) [arXiv:2007.08537 [hep-ph]].
- [21] X. Wang, F. P. Huang and X. Zhang, JCAP **05**, 045 (2020) doi:10.1088/1475-7516/2020/05/045 [arXiv:2003.08892 [hep-ph]].
- [22] S. Wang, T. Terada and K. Kohri, Phys. Rev. D **99**, no.10, 103531 (2019) [erratum: Phys. Rev. D **101**, no.6, 069901 (2020)]
- [23] Y. F. Cai, C. Chen, X. Tong, D. G. Wang and S. F. Yan, Phys. Rev. D **100**, no.4, 043518 (2019)
- [24] Y. F. Cai, C. Lin, B. Wang and S. F. Yan, Phys. Rev. Lett. **126**, no.7, 071303 (2021)
- [25] Y. F. Cai, J. Jiang, M. Sasaki, V. Vardanyan and Z. Zhou, Phys. Rev. Lett. **127**, no.25, 251301 (2021)
- [26] Z. Zhou, J. Jiang, Y. F. Cai, M. Sasaki and S. Pi, Phys. Rev. D **102**, no.10, 103527 (2020)
- [27] I. Y. Kobzarev, L. B. Okun and M. B. Voloshin, Sov. J. Nucl. Phys. **20**, 644 (1975) [Yad. Fiz. **20**, 1229 (1974)].
- [28] S. R. Coleman, Phys. Rev. D **15**, 2929 (1977) Erratum: [Phys. Rev. D **16**, 1248(E) (1977)].
- [29] S. R. Coleman and F. De Luccia, Phys. Rev. D **21**, 3305 (1980).
- [30] S. J. Parke, Phys. Lett. **121B**, 313 (1983).
- [31] K. M. Lee and E. J. Weinberg, Phys. Rev. D **36**, 1088 (1987).
- [32] B. H. Lee and W. Lee, Class. Quant. Grav. **26**, 225002 (2009) [arXiv:0809.4907 [hep-th]].
- [33] B. H. Lee, C. H. Lee, W. Lee and C. Oh, Phys. Rev. D **82**, 024019 (2010) [arXiv:0910.1653 [hep-th]].
- [34] Y. l. Zhang, R. Saito, D. h. Yeom and M. Sasaki, JCAP **1402**, 022 (2014) doi:10.1088/1475-7516/2014/02/022 [arXiv:1312.0709 [hep-th]].
- [35] A. Joti, A. Katsis, D. Loupas, A. Salvio, A. Strumia, N. Tetradis and A. Urbano, JHEP **1707**, 058 (2017) doi:10.1007/JHEP07(2017)058 [arXiv:1706.00792 [hep-ph]].
- [36] N. W. K. Wong, J. Gong, Y. K. Lim and Q. h. Wang, Class. Quant. Grav. **35**, no. 4, 045016 (2018) doi:10.1088/1361-6382/aaa4ea [arXiv:1708.02689 [gr-qc]].

- [37] V. Branchina, F. Contino and A. Pilaftsis, *Phys. Rev. D* **98**, no. 7, 075001 (2018) doi:10.1103/PhysRevD.98.075001 [arXiv:1806.11059 [hep-ph]].
- [38] T. Markkanen, A. Rajantie and S. Stopyra, *Front. Astron. Space Sci.* **5**, 40 (2018) doi:10.3389/fspas.2018.00040 [arXiv:1809.06923 [astro-ph.CO]].
- [39] S. F. Bramberger, M. Chitishvili and G. Lavrelashvili, *Phys. Rev. D* **100**, no. 12, 125006 (2019) doi:10.1103/PhysRevD.100.125006 [arXiv:1906.07033 [gr-qc]].
- [40] A. H. Guth, *Phys. Rev. D* **23**, 347 (1981) [*Adv. Ser. Astrophys. Cosmol.* **3**, 139 (1987)].
- [41] K. Sato, *Mon. Not. Roy. Astron. Soc.* **195**, 467 (1981).
- [42] S. W. Hawking and I. G. Moss, *Phys. Lett.* **110B**, 35 (1982) [*Adv. Ser. Astrophys. Cosmol.* **3**, 154 (1987)].
- [43] D. La and P. J. Steinhardt, *Phys. Rev. Lett.* **62**, 376 (1989)
- [44] Z. Zhou, J. Yan, A. Addazi, Y. F. Cai, A. Marciano and R. Pasechnik, *Phys. Lett. B* **812**, 136026 (2021)
- [45] B. Imtiaz, Y. F. Cai and Y. Wan, *Eur. Phys. J. C* **79**, no.1, 25 (2019)
- [46] A. D. Linde, *Phys. Lett.* **100B**, 37 (1981).
- [47] A. D. Linde, *Nucl. Phys. B* **216**, 421 (1983) Erratum: [*Nucl. Phys. B* **223**, 544 (1983)].
- [48] V. A. Berezin, V. A. Kuzmin and I. I. Tkachev, *Phys. Lett. B* **207**, 397 (1988).
- [49] V. A. Berezin, V. A. Kuzmin and I. I. Tkachev, *Phys. Rev. D* **43**, R3112-3116 (1991)
- [50] R. Gregory, I. G. Moss and N. Oshita, *JHEP* **2007**, 024 (2020) [arXiv:2003.04927 [hep-th]].
- [51] S. R. Coleman, V. Glaser and A. Martin, *Commun. Math. Phys.* **58**, 211 (1978).
- [52] A. D. Linde, *Rept. Prog. Phys.* **42**, 389 (1979).
- [53] E. W. Kolb and M. S. Turner, *Ann. Rev. Nucl. Part. Sci.* **33**, 645 (1983).
- [54] V. A. Kuzmin, V. A. Rubakov and M. E. Shaposhnikov, *Phys. Lett.* **155B**, 36 (1985).
- [55] C. Grojean, G. Servant and J. D. Wells, *Phys. Rev. D* **71**, 036001 (2005) [hep-ph/0407019].
- [56] D. Bodeker, L. Fromme, S. J. Huber and M. Seniuch, *JHEP* **0502**, 026 (2005) [hep-ph/0412366].
- [57] D. E. Morrissey and M. J. Ramsey-Musolf, *New J. Phys.* **14**, 125003 (2012) [arXiv:1206.2942 [hep-ph]].

- [58] K. P. Xie, L. Bian and Y. Wu, JHEP **12**, 047 (2020) doi:10.1007/JHEP12(2020)047 [arXiv:2005.13552 [hep-ph]].
- [59] K. P. Xie, JHEP **02**, 090 (2021) doi:10.1007/JHEP02(2021)090 [arXiv:2011.04821 [hep-ph]].
- [60] M. B. Hindmarsh, M. Luben, J. Lumma and M. Pauly, SciPost Phys. Lect. Notes **24**, 1 (2021) [arXiv:2008.09136 [astro-ph.CO]].
- [61] S. W. Hawking, I. G. Moss and J. M. Stewart, Phys. Rev. D **26**, 2681 (1982).
- [62] Z. C. Wu, Phys. Rev. D **28**, 1898 (1983).
- [63] M. C. Johnson, H. V. Peiris and L. Lehner, Phys. Rev. D **85**, 083516 (2012) [arXiv:1112.4487 [hep-th]].
- [64] D. i. Hwang, B. H. Lee, W. Lee and D. h. Yeom, JCAP **1207**, 003 (2012) [arXiv:1201.6109 [gr-qc]].
- [65] D. I. Hwang, B. H. Lee, W. Lee and D. H. Yeom, Nucl. Phys. B Proc. Suppl. **246-247**, 196-202 (2014)
- [66] C. L. Wainwright, M. C. Johnson, H. V. Peiris, A. Aguirre, L. Lehner and S. L. Liebling, JCAP **1403**, 030 (2014) [arXiv:1312.1357 [hep-th]].
- [67] J. W. York, Jr., Phys. Rev. Lett. **28**, 1082 (1972).
- [68] G. W. Gibbons and S. W. Hawking, Phys. Rev. D **15**, 2752 (1977).
- [69] C. G. Callan, Jr. and S. R. Coleman, Phys. Rev. D **16**, 1762 (1977).
- [70] A. Strumia and N. Tetradis, JHEP **9911**, 023 (1999) [hep-ph/9904357].
- [71] J. Baacke and G. Lavrelashvili, Phys. Rev. D **69**, 025009 (2004) [hep-th/0307202].
- [72] G. V. Dunne and H. Min, Phys. Rev. D **72**, 125004 (2005) [hep-th/0511156].
- [73] D. A. Samuel and W. A. Hiscock, Phys. Lett. B **261**, 251 (1991).
- [74] D. A. Samuel and W. A. Hiscock, Phys. Rev. D **44**, 3052 (1991).
- [75] A. R. Brown, Phys. Rev. D **97**, no. 10, 105002 (2018) [arXiv:1711.07712 [hep-th]].
- [76] A. Masoumi and E. J. Weinberg, Phys. Rev. D **86**, 104029 (2012) [arXiv:1207.3717 [hep-th]].
- [77] M. S. Turner, E. J. Weinberg and L. M. Widrow, Phys. Rev. D **46**, 2384 (1992).

- [78] D. H. Kim, B. H. Lee, W. Lee, J. Yang and D. h. Yeom, Eur. Phys. J. C **75**, no. 3, 133 (2015) [arXiv:1410.4648 [gr-qc]].
- [79] J. R. Bond, J. Braden and L. Mersini-Houghton, JCAP **1509**, 004 (2015) doi:10.1088/1475-7516/2015/09/004 [arXiv:1505.02162 [astro-ph.CO]].
- [80] A. Nakonieczna, Ł. Nakonieczny and D. h. Yeom, Int. J. Mod. Phys. D **28**, no.03, 1930006 (2018) [arXiv:1805.12362 [gr-qc]].
- [81] A. Kosowsky and M. S. Turner, Phys. Rev. D **47**, 4372 (1993) [astro-ph/9211004].
- [82] M. Maggiore, “Gravitational Waves. Vol. 1: Theory and Experiments,” Oxford University Press, 2007.
- [83] S. J. Huber and T. Konstandin, JCAP **0809**, 022 (2008) [arXiv:0806.1828 [hep-ph]].
- [84] S. Weinberg, “Gravitation and Cosmology : Principles and Applications of the General Theory of Relativity,” John Wiley and Sons, New York (1972).
- [85] M. Kamionkowski, A. Kosowsky and M. S. Turner, Phys. Rev. D **49**, 2837 (1994) [astro-ph/9310044].
- [86] K. Schmitz, Symmetry **12** (2020) no.9, 1477 [arXiv:2005.10789 [hep-ph]].
- [87] C. J. Hogan, Mon. Not. Roy. Astron. Soc. **218**, 629 (1986).
- [88] D. Hwang, F. G. Pedro and D. Yeom, JHEP **09**, 159 (2013) [arXiv:1306.6687 [hep-th]].
- [89] J. Hansen and D. Yeom, JHEP **10**, 040 (2014) [arXiv:1406.0976 [hep-th]].
- [90] J. Hansen and D. Yeom, JCAP **09**, 019 (2015) [arXiv:1506.05689 [hep-th]].
- [91] D. Hwang and D. Yeom, Class. Quant. Grav. **27**, 205002 (2010) [arXiv:1002.4246 [gr-qc]].
- [92] D. Hwang, B. H. Lee and D. Yeom, JCAP **12**, 006 (2011) [arXiv:1110.0928 [gr-qc]].
- [93] P. Chen and D. Yeom, JCAP **10**, 022 (2015) [arXiv:1506.06713 [gr-qc]].
- [94] S. E. Hong, D. Hwang, E. D. Stewart and D. Yeom, Class. Quant. Grav. **27**, 045014 (2010) [arXiv:0808.1709 [gr-qc]].
- [95] J. Hansen, D. Hwang and D. Yeom, JHEP **11**, 016 (2009) [arXiv:0908.0283 [gr-qc]].
- [96] D. Hwang and D. Yeom, Class. Quant. Grav. **28**, 155003 (2011) [arXiv:1010.3834 [gr-qc]].
- [97] D. Hwang, B. H. Lee and D. Yeom, JCAP **01**, 005 (2013) [arXiv:1210.6733 [gr-qc]].

- [98] C. Caprini, D. G. Figueroa, R. Flauger, G. Nardini, M. Peloso, M. Pieroni, A. Ricciardone and G. Tasinato, *JCAP* **11**, 017 (2019) doi:10.1088/1475-7516/2019/11/017 [arXiv:1906.09244 [astro-ph.CO]].
- [99] T. Robson, N. J. Cornish and C. Liu, *Class. Quant. Grav.* **36**, no.10, 105011 (2019) doi:10.1088/1361-6382/ab1101 [arXiv:1803.01944 [astro-ph.HE]].
- [100] M. R. Adams and N. J. Cornish, *Phys. Rev. D* **89**, no.2, 022001 (2014) doi:10.1103/PhysRevD.89.022001 [arXiv:1307.4116 [gr-qc]].